Case Studies in Thermal Engineering 34 (2022) 102062

Contents lists available at ScienceDirect

Case Studies in Thermal Engineering

journal homepage: www.elsevier.com/locate/csite

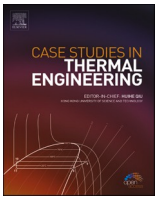

Bioconvection attribution for effective thermal transportation of upper convicted Maxwell nanofluid flow due to an extending cylindrical surface☆

Amna Mariam [a], Imran Siddique [b,*], Sohaib Abdal [a,c], Fahd Jarad [d,e,f,**], Rifaqat Ali [g], Nadeem Salamat [a], Sajjad Hussain [h]

[a] Department of Mathematics, Khwaja Fareed University of Engineering and Information Technology, Rahim Yar Khan, Pakistan
[b] Department of Mathematics, University of Management and Technology, Lahore, 54770, Pakistan
[c] School of Mathematics, Northwest University, No.229 North Taibai Avenue, Xi'an, 7100069, China
[d] Department of Mathematics, Cankaya University, Etimesgut, Ankara, Turkey
[e] Department of Mathematics, King Abdulaziz University, Jeddah, Saudi Arabia
[f] Department of Medical Research, China Medical University Hospital, China Medical University, Taichung, Taiwan
[g] Department of Mathematics, College of Science and Arts, King Khalid University, Muhayil, 61413, Abha, Saudi Arabia
[h] School of Mathematics, Government Post Graduate College Layyah, Punjab, Pakistan

ARTICLE INFO

Keywords:
Upper convected Maxwell fluid
Nanofluid
Bioconvection
Magnetohydrodynamic
Extending cylindrical surface

ABSTRACT

The growth of compact density heat gadgets demands effective thermal transportation. The option of nanofluid plays a dynamic role in this requirement. This research shows the impact of gyrotactic microorganisms on non-Newtonian fluid (Maxwell fluid) passing on the expanding cylindrical surface. The main objective of the present observation is to determine the heat and mass transportation of Maxwell nanofluid. The convective boundary condition and zero mass flux conditions are incorporated. In mathematical derivation, the approximation of the boundary layer is applied. The primal motivation pertains to exaggerating the thermal transport of heat exchangers in industrial processes. To attain the effects of Brownian motion as well as thermophoresis the Buongiorno nanofluid is utilized. By assimilating suitable transformation, the concluding simultaneous for a non-linear set of equations is tackled numerically by hiring Runge-Kutta procedure. The coding is developed and run in the Matlab environment. The leading partial differential system is converted into an ordinary differential system. The role of emerging parameters is elaborated. Also tangible quantities i.e. Skin friction factor, Nusselt number, Sherwood number, and motile density coefficient are enumerated. An accession in the magnetic field causes depreciation in the velocity profile. Where increment in Schmidt number Sc causes a decrement in Sherwood number. The suitable ranges of parameters where increasing or decreasing behavior becomes smooth are taken as $0.0 \leq M \leq 6.0$, $0.0 \leq \gamma \leq 0.8$, $0.7 \leq Pr \leq 1.0$, $0.1 \leq Nt \leq 0.7$, $0.01 \leq Nb \leq 0.1$, $3.0 \leq Sc \leq 6.0$, $2.0 \leq Lb \leq 7.0$, $0.1 \leq Pe \leq 0.7$ and $1.0 \leq \delta \leq 7.0$. The applications of the current study can be seen in chemical and metallurgical industries, the process of thermo-fluid, power generation, executed via condensers, cooling, and heating in large buildings, transportation, etc.

☆ Fully documented templates are available in the elsarticle package on CTAN.

* Corresponding author.
** Corresponding author. Department of Mathematics, Cankaya University, Etimesgut, Ankara, Turkey.
E-mail addresses: imransmsrazi@gmail.com (I. Siddique), fahd@cankaya.edu.tr (F. Jarad).

https://doi.org/10.1016/j.csite.2022.102062
Received 28 February 2022; Received in revised form 10 April 2022; Accepted 20 April 2022
Available online 25 April 2022

Nomenclature

Latin Symbols

u, v	velocity components(m/s)
z, r	cartesian coordinates(m)
$U_w(r, z)$	stretching velocity(m/s)
B_0	magnetic field strength(T)
C	concentration of nanoparticles
T	temperature of nanoparticles(K)
N	Micro-organisms distribution
K	thermal conductivity(W/m.K)
C_p	effective heat capacity(J/K)
C_s	heat capacity for solid surface(J/K)
D_B	Brownian diffusion coefficient(m^2/s)
D_T	thermophoresis diffusion coefficient(m^2/s)
D_m	diffusivity of microrganisms(m^2/s)
T_∞	ambient temperature(K)
C_∞	ambient concentration of nanoparticles
N_∞	ambient micro-organisms distribution
b	chemotaxis constant(m)
W_c	speed of gyrotactic cell(m/s)
n	rotation of micro-organisms(1/s)
M	Magnetic parameter
Pr	Prandtl number
Nb	Brownian motion parameter
Nt	thermophoresis parameter
Sc	Schimdt number
Lb	bio-convection Lewis number
Pe	Peclet number

Greek Symbols

β	Deborah number
ν	kinematic viscosity(m^2/s)
λ	fluid relaxation time
σ	electrical conductivity(S/m)
ρ	Density(kg/m^3)
γ	curvature parameter
η	similarity variable
θ	similarity temperature
φ	similarity concentration of nanoparticles
χ	similarity density of micro-organisms
δ	microorganisms concentration difference

Subscripts

p	nanoparticles
w	on the cylinder surface
∞	Ambient

1. Introduction

The Maxwell fluid model was formulated with the help of Hookean springs in combination with a buffer designed to mechanically describe viscoelastic materials. Firstly, Maxwell fluid model was given by Maxwell [1] to discuss the behavior of air due to visco-elasticity. The basic elements of different arrangements can be combined to show more complex behavior of viscoelasticity. An essential property of Maxwell fluids is that they exhibit relaxation of stress. The literature shows that many efforts have been made to study the effects of rheology on Maxwell fluids having various geometries in the boundary layer of hydrodynamics. Firstly, Olsson and Ystrom [2] investigated the characteristics of Maxwell fluid along with the upper convective viscoelasticity. Reddy et al. [3] elaborate Cattaneo–Christov heat flux effects for Maxwell fluid with the inclusion of nanoparticles. Sreedevi et al. [4] discussed the effects of Brownian motion and thermophoresis on 3-D Maxwell flow. Mahsud et al. [5] discuss the flow of the boundary layer for Maxwell fluid

which is formulated by the time-fractional derivatives of Caputo-Fabrizio along with an upper-convected. They observed that the flow of fractional fluids is slower than common fluids. Ullah et al. [6] analyzed the creeping flow of Maxwell fluids having a slit that is porous along with continuous absorption with the wall slip. Fetecau et al. [7] investigated the flow of Maxwell fluid in a porous plate along with mathematical reasoning, which was influenced by the accelerating wall. Zhao [8] demonstrated the convection, magnetic field, and velocity slip of part of the fluid's peristaltic motion. Wang et al. [9] have established analytical expressions for the solutions of steady-state for oscillating motions of incompressible Maxwell fluids which are passing through a channel along with a rectangular or isosceles right-angled triangle cross-section. Abdal et al. [10] used living microorganisms to elaborate on the effects of activation energy of Williamson Maxwell nanofluid flow.

Magnetohydrodynamics (MHD) is the discussion of conductive fluids, such as saltwater, electrolytes, plasmas, and liquid metals. Firstly, this term was introduced by Alfven [11]. Such fluids have many engineering as well as industrial applications, i.e. crystal growth, cooling in reactors, targeting the magnetic drug, MHD sensors, and generation of power. Dependency of MHD contains magnetic flux density. Saeed and Gul [12] studied the relocation of mass and heat of MHD Casson nanofluids flowing through a plate that is in motion. Jawad et al. [13] mathematically demonstrated the Maxwell MHD flow which is dependent on time along with nanofluids through the stretched surface. This can be useful in the field of food processing, transportation of biological fluids, drilling of oil, pharmaceutical, manufacturing of drugs, and coating rheology [14]. In order to adequately capture the different properties of non-Newtonian fluids, due to the different properties of the fluid, many theories, as well as models, have been published to elaborate on their flow [15,16]. Ali et al. [17] discussed magnetohydrodynamics effects on the nanofluid flow. Similar work was done with different numerical schemes by Refs. [18–20].

In various systems, there is a great importance of nanofluids due to the heat transfer. Its applications do not matter due to the presence of limited stocks of energy gadgets. Nanofluids has great importance in medical, physiological state, etc. The excellent storage of thermal energy and the greater coefficient of physical properties of the transmitted thermos is very basic aspects of the flow of nanofluids. Mostly, fluids having equitable thermal conductivity as well as water, oil, and relocation of heat are used for its energy and transformation. Due to the advancement in nanostructures firstly, a Chinese researcher Choi et al. [21] proposed a new fluid which was named by nano liquids. Huang et al. [22] assembled nano-particles into the required shapes that have fascinated the extensive attention. This type of architectures does not depend only on the properties of nano particles in building blocks, it also depends on the component's geometry to attain unique results beyound the composition. Sami et al. [23] analyzed a high quality supplement which may be used for cereals as well as grains is mushroom. Rokayya et al. [24] investigated the effect of nano fluids their mechanical characteristics as well as chemical changes on the mushrooms with white buttom during the storage. Li et al. [25] investigated on the use of nano-materials for the safety and assessment of blueberry fruits along with chitosan. Yi et al. [26] There are a lots of processes are developed for the advance control of integration. For example with the help of colloidal self-assembly, modification in different nanoparticles can be organized with the help of assembly forces. Sreedevi et al. [27]studied magnetic field and thermal radiation effect by using Tiwari-Das nanofluid model. Sudarsana et al. [28] used zero mass flux conditions on the flow of nanofluids. Abro et al. [29] experimental investigated mild steel. Alarifi et al. [30] analytically performed the quality assurance of impact-damaged laminate composite structures. Further, Asmatulu et al. [31] investigated the effects of surface treatments on carbon fiber-reinforced composite laminates. Abdal et al. [32] used temperature conditions PST and PHF on micropolar based nanofluid. Many researchers were done similar work on nanofluid [33–39].

Due to the increment in the density of self-propelled kinetic microorganisms in a definite direction of normal liquid occurrence of bioconvection is done. Where the density gets increases in moving fluid. Magnetic field shows great effect on the processes of relocation of mass and heat in the fluids which is electrically conductive. It is very helpful in the treatment of arterial diseases, blood flow reduction during surgeries, drawing of copper wires, etc. Different biological sciences holds physical applications of it, such as enzymatic biosensors, biofuels, enzymes, transport processes, microsystems, biotechnology, biological tissues, bacteria, etc. It depends on the cumulative use of nutrients as well as microorganisms in the oil region to investigate the variation of permeability. Khan et al. [40] investigated the flow of bioconvection along with nanofluid having gyrotactic microorganisms. Nima et al. [41] discussed the flow of boundary layer in a vertical strong flat plate induced in a Darcian medium which is porous having gyrotactic microorganisms. Nayake et al. [42] studied the exponential development of the flow velocity of Casson fluid along with electromagnetic sheet during the sliding effects of nanofluid which has chemical, thermal, isolation, and mobile microbial effects in it. Mansour et al. [43] numerically elaborated the study of magneto-hydrodynamic convection as well as Gyro-Organism in a cave which is shape of closed-loop. Balla et al. [44] investigated the activity of microorganisms along with nanofluids in the square hole which is porous. Khan et al. [45] studied the bioconvection in the fluid flow of nanofluids having the continued Oldroyd-B walls.

The exceeding heat transportation in compact equipment is a serious matter in the research field of thermal engineering. In comparison to the fin and fan extensions, nanofluid dynamics are becoming a popular concept. There seemed a gap to differentiate the characteristics of viscous nanofluid and viscoelastic (upper convected Maxwell) nanofluids' heat and mass transport owing to an extending cylindrical surface (see Saif et al. [46]). Moreover, the probable settling of nano entities is addressed with the bioconvection of gyrotactic microorganisms. The findings of this study are relevant to different thermal transportation-related dynamics of rockets and missiles. There are many applications that can be observed such as chemical and metallurgical industries, process of thermo-fluid, power generation, executed via condensers, cooling and heating in large buildings, transportation etc.

2. Flow assumptions and formulation

Consider a flow of viscoelastic fluids in two dimensions that obeys the Maxwell model, and it is developed through a stretched cylindrical surface of radius R. According to the geometry of the problem, the z-axis is along the axial direction and r is the radial

coordinate. Assumed that the cylinder is expanding axially having velocity $u = U_o\left(\frac{z}{l}\right)$, where U_o represents the reference velocity, as well as l, denotes its characteristics length (see Fig. 1). The fluid is assumed to be electrically conducting and a magnetic field is fixed normal to the axis of the cylinder. During the melting mechanism of the cylindrical surface, the transfer of heat is initiated. So, the considered assumption is $T_m < T_\infty$ where T_m denotes the melting temperature of the surface and T_∞ is the asymptotic value for the temperature. A mild homogenous emulsion of nanoparticles is assumed with a volume concentration of C. In addition, a mixture of self-motivated microorganisms of concentration N exists independent of nano-entities. The origin is fixed and there are two equal and opposite forces acting on it.

Flow model for the given problem is [46,47]:

$$\frac{\partial(ru)}{\partial z} + \frac{\partial(rv)}{\partial r} = 0 \tag{1}$$

$$u\left(\frac{\partial u}{\partial z}\right) + v\left(\frac{\partial u}{\partial r}\right) = v\left(\frac{1}{r}\frac{\partial u}{\partial r} + \frac{\partial^2 u}{\partial r^2}\right) + \frac{\lambda}{\rho}\left(v^2\frac{\partial^2 u}{\partial r^2} + 2uv\frac{\partial^2 u}{\partial r \partial z} + u^2\frac{\partial^2 u}{\partial z^2}\right) - \frac{\sigma B_o^2}{\rho}u \tag{2}$$

$$u\left(\frac{\partial T}{\partial z}\right) + v\left(\frac{\partial T}{\partial r}\right) = \frac{K}{\rho C_p}\left(\frac{1}{r}\frac{\partial T}{\partial r}\frac{\partial^2 T}{\partial r^2}\right) + \tau\left(D_B\frac{\partial T}{\partial r}\frac{\partial C}{\partial r} + \frac{D_T}{T_\infty}\left(\frac{\partial T}{\partial y}\right)^2\right) \tag{3}$$

$$u\left(\frac{\partial C}{\partial z}\right) + v\left(\frac{\partial C}{\partial r}\right) = D_B\left(\frac{1}{r}\frac{\partial C}{\partial r}\frac{\partial^2 C}{\partial r^2}\right) + \frac{D_T}{T_\infty}\left(\frac{1}{r}\frac{\partial T}{\partial r}\frac{\partial^2 T}{\partial r^2}\right) \tag{4}$$

$$u\left(\frac{\partial N}{\partial z}\right) + v\left(\frac{\partial N}{\partial r}\right) + \left(\frac{N}{r}\frac{\partial C}{\partial r} + \frac{\partial N}{\partial r}\frac{\partial C}{\partial r} + N\frac{\partial^2 C}{\partial r^2}\right)\frac{bW_c}{(C_m - C_\infty)} = D_m\left(\frac{\partial^2 N}{\partial r^2} + \frac{1}{r}\frac{\partial N}{\partial r}\right) \tag{5}$$

Subjected to the constraints [48,49]:

$$u(r,z) = U_w(r,z) = U_o\left(\frac{z}{l}\right), v(r,z) = 0,\ -k_f\frac{\partial T}{\partial r} = h_f(T_w - T), D_B\frac{\partial C}{\partial r} + \frac{D_T}{T_\infty}\frac{\partial T}{\partial r} = 0,\ N(r,z) = N_w,\ at\ r = R \tag{6}$$

$$u(r,z) \to 0,\ v(r,z) \to 0,\ T(r,z) \to T_\infty,\ C(r,z) \to C_\infty,\ N(r,z) \to N_\infty\ as\ r \to \infty \tag{7}$$

Here (u, v) indicates the velocities for radial and axial symmetries, λ denotes the time for relaxation, the density of fluid is represented by ρ, k, T, C_p, and C_s represents thermal conductivity, temperature, heat capacity, capacity of heat for solid surface.

Similarity transformations are given below:

$$\eta = \frac{r - R}{2R}\sqrt{\frac{U_o}{vl}},\ u = \frac{U_o z}{l}f'(\eta),\ v = -\frac{R}{r}\sqrt{\frac{U_o v}{l}}f(\eta), \tag{8}$$

$$\theta(\eta) = \frac{T - T_\infty}{T_w - T_\infty},\ \varphi(\eta) = \frac{C - C_\infty}{C_w - C_\infty},\ \chi(\eta) = \frac{N - N_\infty}{N_w - N_\infty} \tag{9}$$

The above equations are converted as:

$$(1 + 2\gamma\eta)f''' + 2\gamma f'' + ff'' - f'^2 + \frac{1}{\rho}\frac{\gamma\beta}{(1 + 2\gamma\eta)}f^2 f' - \frac{2\beta}{\sqrt{(1 + 2\gamma\eta)}}ff'f'' + \frac{\beta}{\rho}f^2 f'' - Mf' = 0 \tag{10}$$

$$(1 + 2\gamma\eta)\theta'' + 2\gamma\theta' + Pr\theta' f + NbPr(1 + 2\gamma\eta)\theta'\varphi' + NtPr(1 + 2\gamma\eta)\theta'^2 = 0 \tag{11}$$

$$(1 + 2\gamma\eta)\varphi'' + \frac{Nt}{Nb}(1 + 2\gamma\eta)\theta'' + \frac{Nt}{Nb}\gamma\theta' + 2\gamma\varphi' - Scf\varphi' = 0 \tag{12}$$

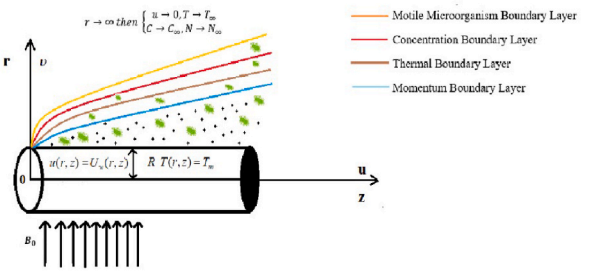

Fig. 1. Flowchart.

$$(1+2\gamma\eta)\chi'' + 2\gamma\chi' - Lb\chi f' + Lb\chi' - Pe((\varphi'(1+2\gamma\eta) + 2\gamma\varphi'\theta'\varphi')(\chi+\delta) + (1+2\gamma\eta)\chi'\varphi') = 0 \tag{13}$$

The boundary conditions (6) and (7) are transformed as:

$$f'(0) = 1, f(0) = 0, \theta'(0) = -B_i(1-\theta(0)), Nb\varphi'(0) + Nt\theta'(0) = 0, \chi(0) = 1, \tag{14}$$

$$f'(\infty) \to 0,\ \theta(\infty) \to 0,\ \varphi(\infty) \to 0,\ \chi(\infty) \to 0. \tag{15}$$

In the above $\beta = \frac{\lambda U_o}{l}$ is Deborah number, $\gamma = \sqrt{\frac{\nu l}{U_o R^2}}$ is known as curvature parameter, Prandtl number is $Pr = \frac{\nu}{\alpha}$, $Nb = \frac{\tau D_B (C_w - C_\infty)}{\nu}$ is the Brownian motion parameter, $Nt = \frac{\tau D_T (T_w - T_\infty)}{T_\infty}$ is the Thermophoresis parameter, $Lb = \frac{\nu}{D_m}$ is the bioconvection lewis number, Peclet number is $Pe = \frac{bW_c}{D_m}$, Microorganisms difference parameter is $\delta = \frac{N_\infty}{(N_w - N}$ and $Sc = \frac{\nu}{D_B}$ is Schmidt number.

The physical quantities are defined as [37,46]:

$$\frac{1}{2}Cf_z Re_z^{\frac{1}{2}} = \frac{\tau_{rz}}{\rho U_w^2},\ Nu_z = \frac{zq_w}{\kappa(T_w - T_\infty)},\ Shr_z = \frac{zq_m}{D_B(C_w - C_\infty)},\ \ Nr_z = \frac{zq_r}{D_m(N_w - N_\infty)}. \tag{16}$$

Thus we have.

$C_f(Re_x)^{-1/2} = f''(0)$, $Nu_x(Re_x)^{-1/2} = -\theta'(0)$, $Sh_x(Re_x)^{-1/2} = -\varphi'(0)$, $Nn_x(Re_x)^{-1/2} = -\chi'(0)$,Where, $(Re_x) = \frac{xU_w}{\nu}$ is the local Reynolds number.

3. Solution procedure

The system of equations (10)-(13) along with the boundary constraints (14) and (15) is solved with the shooting technique. This compound set of non-linear equations requires simultaneous solutions. Such problems are better to be resolved numerically because their closed form solutions are extremely difficult. Beside the other methods such as FDM, FEM, Runge-Kutta method is very economical and reliable to yields results. In order to develop a coding of the procedure, a system of first order differential equations in attained as follows:

$y_1' = y_2$

$y_2' = y_3$

$y_3' = \left(\frac{-1}{(1+2\gamma\eta)+\frac{\beta}{\rho}y_1^2}\right)\left(2\gamma y_3 + y_1 y_3 + \frac{\gamma\beta y_1^2 y_3}{\rho(1+2\gamma\eta)} - y_2^2 - \frac{2\beta}{\sqrt{(1+2\gamma\eta)}}y_1 y_2 y_3 - My_2\right)$

$y_4' = y_5$

$y_5' = \left(\frac{-1}{(1+2\gamma\eta)}\right)(2\gamma y_3 + Pry_1 y_5 + NbPr(1+2\gamma\eta)y_5 y_7 + NtPr(1+2\gamma\eta)y_5^2)$

$y_6' = y_7$

$y_7' = \left(\frac{-1}{(1+2\gamma\eta)}\right)\left(\frac{Nt}{Nb}(1+2\gamma\eta)y_5' + \frac{Nt}{Nb}\gamma y_5 + 2\gamma y_7 - Scy_1 y_7\right)$

$y_8' = y_9$

$y_9' = \left(\frac{-1}{(1+2\gamma\eta)}\right)(2\gamma y_9 - Lby_2 y_8 + Lby_9 - Pe((y_7'(1+2\gamma\eta) + 2\gamma y_7)(y_8+\delta_1) + (1+2\gamma\eta)y_7 y_9))$

While the relation in eq (12) are given as:

$y_2(0) = 1$, $y_1(0) = 0$, $y_4(0) = (1+y_5)(1/B_i)$, $Nby_7 + Nty_5 = 0$, $y_9 = 1$,

$y_2(\infty) \to 0$, $y_4(\infty) \to 1$, $y_4(\infty) \to 0$, $y_6(\eta) \to 0$, $y_8(\eta) \to 0$.

4. Results and discussion

For the validation of current results, these are compared with some previous numerical studies as limiting cases to be enlisted in Table 1 (see Refs. [46,50–52]). Here, the results are compared for various values of curvature parameter γ. There seems a good correlation among the results. After gaining confidence in the numerical procedure, an extensive computational effort is carried out to disclose to the impact of sundry parameters on the velocity $f'(\eta)$, skin friction factor $-f''(0)$, temperature $\theta(\eta)$, Nusselt number $-\theta'(0)$, nanoparticle volume friction $\varphi(\eta)$, Sherwood number $-\varphi'(0)$, microorganism distribution function $\chi(\eta)$ and density function $-\chi'(0)$. The graphical results are presented for two situations (i) viscous nanofluids ($\beta = 0$) (ii) UCM nanofluids ($\beta \neq 0$).

Graphical outcomes are obtained for different parameters when $M = 0.5$, $\beta = 0.1$, $\gamma = 0.1$, Pr = 0.7, $Nt = 0.1$, $Sc = 3.0$, $Nb = 0.1$, $Pe = 0.1$, Lb = 1.0, $\delta = 1$. The effect of curvature γ, as well as magnetic parameter M, is illustrated in Fig. 2. Axillary flow expands in the

Table 1
Comparative study for γ.

γ	Saif et al. [46]	Hashim et al. [50]	Poply et al. [51]	Rangi and Naseem [52].	Our results
0.00	−1.000000	−1.000000	–	−1.000000	−1.000000
0.10	−1.037231	−1.036979	−1.036977	–	−1.038081
0.25	−1.094951	−1.094373	–	−1.094378	−1.095154
0.30	−1.111219	−1.111165	−1.111138	–	−1.111501

boundary layer by incrementing the curvature parameter γ. On the other hand, an accession in the value of M causes a depreciation in the velocity. It is because of reactive and resistive force (Lorentz force). The thickness of the boundary layer is narrowed. Thus, decrement in velocity can be seen due to the enhancement in drag force by increasing the value of M. These figures convince that the speed of non-Newtonian nanofluid ($\beta = 0$) is slower in comparison to that of viscous nanofluid ($\beta \neq 0$). Physically, the viscous effects for non-Newtonian fluid are stronger. Fig. 3, shows the enhancement in curvature parameter γ causes arise in the temperature $\theta(\eta)$. It is due to the reduction in the thickness of boundary layer thermally with incrementing values of γ. Similarly, an accession in magnetic parameter M which diminishes the temperature $\theta(\eta)$. Physically, the effect of magnetic field generates a resistance force (Lorentz force) as well as it supports and increases the thickness of thermal boundary layer. In Fig. 4, rising trend is observed in $\theta(\eta)$ when Nt (thermophoresis parameter) is boosted up. The reason is that as the particles get heat and start moving with more kinetic energy and pulled away from cold to hotter region. But incrementing the values of Prandtl number Pr, temperature $\theta(\eta)$ goes down due to depreciation in thermal diffusivity. Basic reason for the retardation in temperature is that Prandtl number Pr has inverse relation with thermal diffusivity. Fig. 5 is displayed to show the effect of concentration profile $\varphi(\eta)$ due to variation of M and γ. The concentration $\varphi(\eta)$ increases when M has larger values. Physically, the increment in M shows an accession in drag force which causes an increase in concentration profile $\varphi(\eta)$. While by increasing the value of γ causes an increment in the concentration profile $\varphi(\eta)$ too. By increasing the values of curvature γ corresponds to the small amount of surface area of cylinder. It causes to reduce the resistance due to which concentration profile $\varphi(\eta)$ increases. Fig. 6 elaborates that with increasing values of Schmidt number Sc, the concentration profile $\varphi(\eta)$ decreases. It is due to the inverse relation of mass diffusivity with Schmidt number. So greater value of Sc causes a depreciation in mass diffusion due to which the concentration of nano particles drops. The effect of Brownian motion parameter Nb on concentration profile $\varphi(\eta)$ can also be observed. It is clear that an accession in Nb causes a decrement in concentration profile $\varphi(\eta)$. Physically, the fluid gets heat up due to the Brownian motion in the boundary layer along with a depreciation in the particles of fluid. Also form these curves it can be observed that concentration profile $\varphi(\eta)$ is said to an increasing function for the incrementing values of Nt. Physically the tiny particles backed out from hotter to cold area in thermophoresis phenomenon. The thermal boundary layer, temperature as well as concentration profile shows increment with constantly heating and the particles gets back from surface. Fig. 7 is desire to elaborates the motile density profile $\chi(\eta)$ for incrementing values of magnetic parameter M. With these curves, it can be observed that an accession in M causes an enhancement in motile density profile $\chi(\eta)$ due to increase in drag force. It can also be observed that with enhancement in curvature parameter γ causes an increase in motile density profile $\chi(\eta)$. In Fig. 8, the motile density profile $\chi(\eta)$ can be said as decreasing function for the bioconvection Lewis number Lb. With increasing the values of Lb, a depreciation in diffusivity in the motile microorganisms due to which motile density profile $\chi(\eta)$ decreases. While by increasing the values of Peclet number i.e. Pe causes a decrease in motile density profile $\chi(\eta)$. Physically, it is due to yielding of rapid motion in the particles of fluid. Due to which the thickness of motile microorganisms reduces. Similarly, by increasing the values of microorganism's difference parameter δ a depreciation in motile density profile $\chi(\eta)$ can be observed. Basically, the strength of particles decreases when microorganisms difference parameter raises which cause reduction in motile density profile.

Table 2 illustrates the alterations in the skin friction against different parameters. An accession in skin friction factor can be observed with the rising values of M, γ and β parameters. Table 3 demonstrates the changings in Nusselt number with respect to various parameters. By increasing the various parameters i.e. γ, Pr and Nt causes an increase in Nusselt number. Table 4 shows the behavior of Sherwood number by variating the parameters i.e. γ, Sc, Nb and Nt. An increment is observed in Sherwood number with the raising values of γ and Nt. Along with a depreciation is examined with the incrementing values of Sc and Nb. By incrementing the values of γ causes an increase in motile density. While a decrement can be observed in motile density with an accession in Pe, Lb and δ is seen in Table 5.

5. Conclusions

A numerical and theoretical study of microorganisms is made for the flow of Maxwell nanofluid. The fluid moves owing to a linear stretch in a stretching cylindrical surface. A comparative analysis for viscous nanofluid and Maxwell nanofluid is presented. The computational procedure is reveals the nature of velocity, temperature and their physical quantities due to variation of influential parameters. The salient finding are outlined as below:

- By incrementing the values of curvature parameter γ, velocity field $f'(\eta)$ shows an accession. Whereas, a decreasing trend can be observed by increasing the values of M.

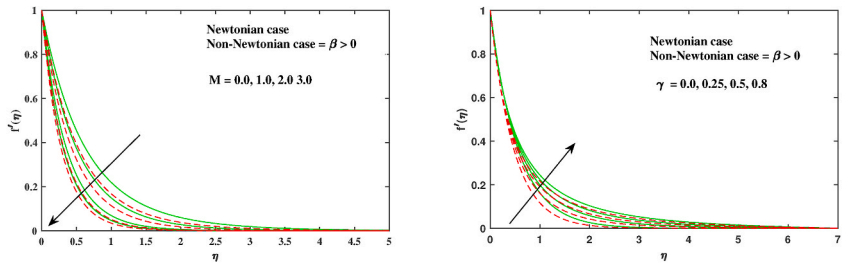

Fig. 2. Fluctuation of $f'(\eta)$ along with M and γ.

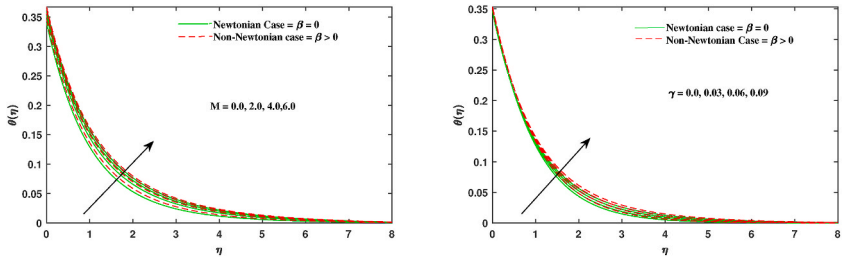

Fig. 3. Fluctuation of $\theta(\eta)$ along with M and γ.

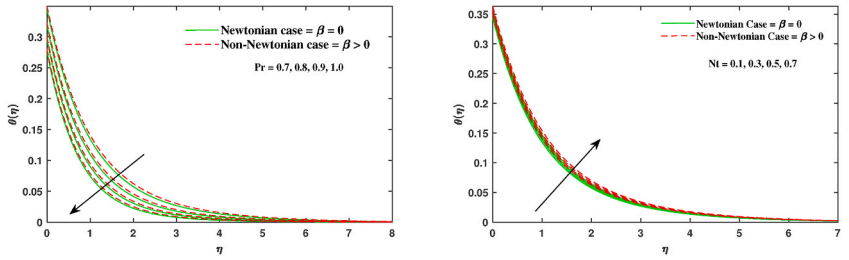

Fig. 4. Fluctuation of $\theta(\eta)$ along with Pr and Nt.

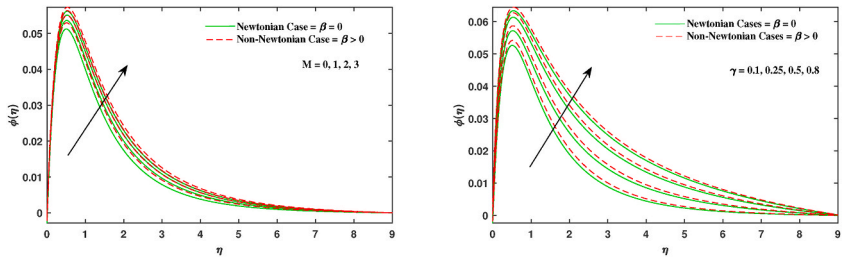

Fig. 5. Fluctuation of $\varphi(\eta)$ along with M and γ.

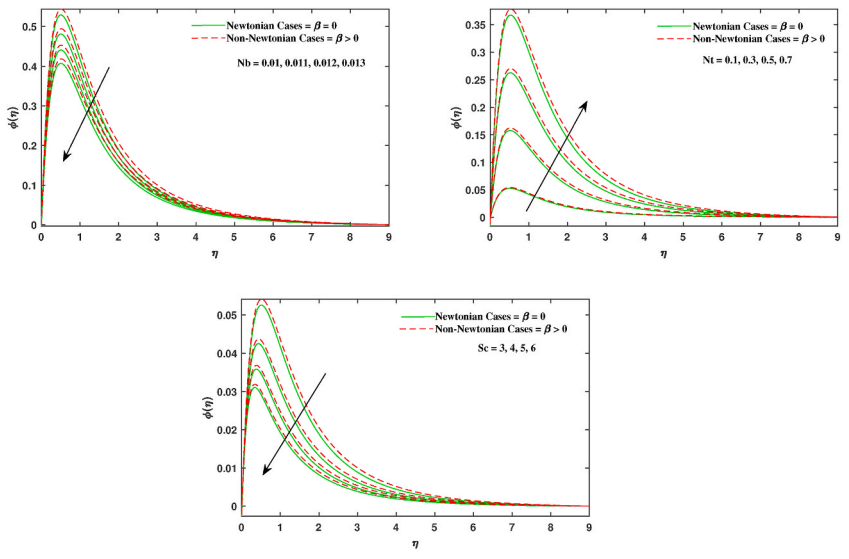

Fig. 6. Fluctuation of $\varphi(\eta)$ along with Nb, Nt and Sc.

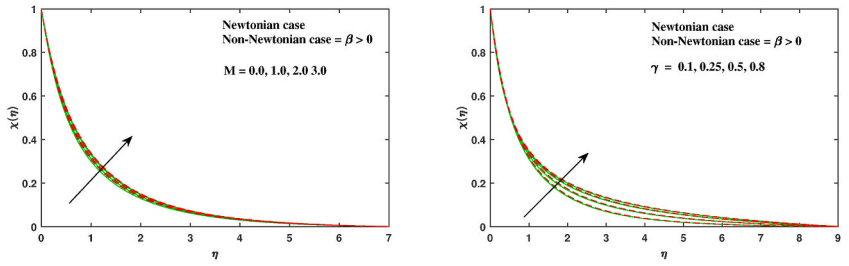

Fig. 7. Fluctuation of $\chi(\eta)$ along with M and γ.

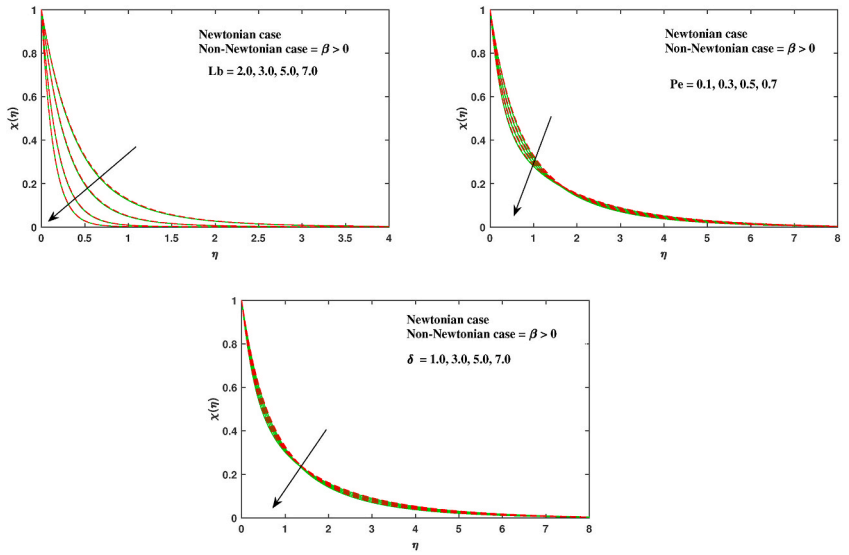

Fig. 8. Fluctuation of $\chi(\eta)$ along with Lb, Pe and δ.

Table 2
Results for Skin friction factor $-f''(0)$.

M	β	γ	$-f''(0)$
0.0	0.1	0.1	1.9542
0.5			2.1665
1.0			2.3494
0.5	0.01		1.8845
	0.05		2.0029
	0.1		2.1665
	0.1	0.1	2.1665
		0.2	2.1931
		0.3	2.2214

Table 3
Results for Nusselt number $-\theta'(0)$.

γ	Pr	Nt	$-\theta'(0)$
0.1	0.7	0.1	0.3280
0.2			0.3305
0.3			0.3337
0.1	0.7		0.3280
	0.9		0.3523
	1.1		0.3702
	0.7	0.01	0.3289
		0.05	0.3285
		0.1	0.3280

Table 4
Results for Sherwood number $-\varphi'(0)$.

γ	Sc	Nb	Nt	$-\varphi'(0)$
0.1	3.0	0.1	0.1	0.3046
0.2				0.3216
0.3				0.3362
0.1	1.0			0.3189
	2.0			0.3090
	3.0			0.3046
	3.0	0.1		0.3046
		0.2		0.1547
		0.3		0.1042
		0.1	0.1	0.3046
			0.2	0.6072
			0.3	0.9078

Table 5
Results for motile density number $-\chi'(0)$.

γ	Pe	Lb	δ	$-\chi'(0)$
0.1	0.1	1.0	1.0	1.3374
0.2				1.3643
0.3				1.3961
0.1	0.1			1.3374
	0.2			1.4809
	0.3			1.6222
	0.1	1.0		1.3374
		2.0		2.3592
		3.0		3.3577
		1.0	1.0	1.3374
			2.0	1.4159
			3.0	1.4945

- Temperature profile $\theta(\eta)$ increases with the increase in γ, M as well as Nt, having the thin region boundary. Also it shows a depreciation in $\theta(\eta)$ with increasing values of Pr.
- An increment in concentration profile $\varphi(\eta)$ can be observed with the increasing values of γ, M and Nt. Also a decrease is caused with the incrementing values of Sc and Nb.
- While motile density profile $\varphi(\eta)$ shows an accession along with the growing values of M and γ. Also it shows a decrement with the raising values of Lb, Pe and δ.
- Skin friction factor $-f''(0)$ rises for sufficiently greater values of M, γ and β.
- The value of Nusselt number $-\theta'(0)$ is raising with the increasing values of γ and Pr. While it a depreciation can be observed with growing values of Nt.
- An accession can be seen in Sherwood number $-\varphi'(0)$ with the raising values of γ and Nt whereas it diminishes by the growing values of Sc and Nb.
- Motile density number show accretion by the growing values of γ, Pe, Lb and δ.

Availability of data and materials

Not applicable.

Funding

Not applicable.

Authors' contributions

Both authors have equal contributions.

Declaration of competing interest

The authors declare that they have no known competing financial interests or personal relationships that could have appeared to influence the work reported in this paper.

Acknowledgement

The authors would like to express the gratitude to Deanship of Scientific Research at King Khalid University, Saudi Arabia for

providing funding research group under the research grant number R.G.P. 2/51/43.

References

[1] J.C. Maxwell, Iv. on the dynamical theory of gases, Phil. Trans. Roy. Soc. Lond. 157 (1867) 49–88.
[2] F. Olsson, J. Ystrom, Some properties of the upper convected maxwell model for viscoelastic fluid flow, J. Non-Newtonian Fluid Mech. 48 (1–2) (1993) 125–145.
[3] P.S. Reddy, P. Sreedevi, Effect of cattaneo–christov heat flux on heat and mass transfer characteristics of maxwell hybrid nanofluid flow over stretching/shrinking sheet, Phys. Scripta 96 (12) (2021), 125237.
[4] P. Sreedevi, P. S. Reddy, Combined influence of brownian motion and thermophoresis on maxwell three-dimensional nanofluid flow over stretching sheet with chemical reaction and thermal radiation, J. Porous Media 23 (4).
[5] Y. Mahsud, N.A. Shah, D. Vieru, Influence of time-fractional derivatives on the boundary layer flow of maxwell fluids, Chin. J. Phys. 55 (4) (2017) 1340–1351.
[6] H. Ullah, D. Lu, A.M. Siddiqui, T. Haroon, K. Maqbool, Hydrodynamical study of creeping maxwell fluid flow through a porous slit with uniform reabsorption and wall slip, Mathematics 8 (10) (2020) 1852.
[7] C. Fetecau, R. Ellahi, S.M. Sait, Mathematical analysis of maxwell fluid flow through a porous plate channel induced by a constantly accelerating or oscillating wall, Mathematics 9 (1) (2021) 90.
[8] J. Zhao, Axisymmetric convection flow of fractional maxwell fluid past a vertical cylinder with velocity slip and temperature jump, Chin. J. Phys. 67 (2020) 501–511.
[9] S. Wang, P. Li, M. Zhao, Analytical study of oscillatory flow of maxwell fluid through a rectangular tube, Phys. Fluids 31 (6) (2019), 063102.
[10] S. Abdal, I. Siddique, D. Alrowaili, Q. Al-Mdallal, S. Hussain, Exploring the magnetohydrodynamic stretched flow of williamson maxwell nanofluid through porous matrix over a permeated sheet with bioconvection and activation energy, Sci. Rep. 12 (1) (2022) 1–12.
[11] H. Alfvén, Existence of electromagnetic-hydrodynamic waves, Nature 150 (3805) (1942) 405–406.
[12] A. Saeed, T. Gul, Bioconvection casson nanofluid flow together with Darcy-forchheimer due to a rotating disk with thermal radiation and arrhenius activation energy, SN Appl. Sci. 3 (1) (2021) 1–19.
[13] M. Jawad, A. Saeed, T. Gul, Entropy generation for mhd maxwell nanofluid flow past a porous and stretching surface with dufour and soret effects, Braz. J. Phys. 51 (3) (2021) 469–480.
[14] M.G. Reddy, N. Kumar, B. Prasannakumara, N. Rudraswamy, K.G. Kumar, Magnetohydrodynamic flow and heat transfer of a hybrid nanofluid over a rotating disk by considering arrhenius energy, Commun. Theor. Phys. 73 (4) (2021), 045002.
[15] A. Hussain, L. Sarwar, S. Akbar, M. Malik, S. Ghafoor, Model for mhd viscoelastic nanofluid flow with prominence effects of radiation, Heat Tran. Asian Res. 48 (2) (2019) 463–482.
[16] E.O. Fatunmbi, S.S. Okoya, Heat transfer in boundary layer magneto-micropolar fluids with temperature-dependent material properties over a stretching sheet, Adv. Mater. Sci. Eng. 2020 (2020), 5734979.
[17] B. Ali, I. Siddique, A. Shafiq, S. Abdal, I. Khan, A. Khan, Magnetohydrodynamic mass and heat transport over a stretching sheet in a rotating nanofluid with binary chemical reaction, non-fourier heat flux, and swimming microorganisms, Case Stud. Therm. Eng. 28 (2021), 101367.
[18] S. Afzal, I. Siddique, F. Jarad, R. Ali, S. Abdal, S. Hussain, Significance of double diffusion for unsteady carreau micropolar nanofluid transportation across an extending sheet with thermo-radiation and uniform heat source, Case Stud. Therm. Eng. 28 (2021), 101397.
[19] D. Habib, N. Salamat, S. Hussain, B. Ali, S. Abdal, Significance of stephen blowing and lorentz force on dynamics of Prandtl nanofluid via keller box approach, Int. Commun. Heat Mass Tran. 128 (2021), 105599.
[20] U. Habib, S. Abdal, I. Siddique, R. Ali, A comparative study on micropolar, williamson, maxwell nanofluids flow due to a stretching surface in the presence of bioconvection, double diffusion and activation energy, Int. Commun. Heat Mass Tran. 127 (2021), 105551.
[21] S. U. Choi, J. A. Eastman, Enhancing Thermal Conductivity of Fluids with Nanoparticles.
[22] C. Huang, X. Chen, Z. Xue, T. Wang, Effect of structure: a new insight into nanoparticle assemblies from inanimate to animate, Sci. Adv. 6 (20) (2020), eaba1321.
[23] R. Sami, A. Elhakem, M. Alharbi, N. Benajiba, M. Almatrafi, A. Abdelazez, M. Helal, Evaluation of antioxidant activities, oxidation enzymes, and quality of nano-coated button mushrooms (agaricus bisporus) during storage, Coatings 11 (2) (2021) 149.
[24] S. Rokayya, E. Khojah, A. Elhakem, N. Benajiba, M. Chavali, K. Vivek, A. Iqbal, M. Helal, Investigating the nano-films effect on physical, mechanical properties, chemical changes, and microbial load contamination of white button mushrooms during storage, Coatings 11 (1) (2021) 44.
[25] Y. Li, S. Rokayya, F. Jia, X. Nie, J. Xu, A. Elhakem, M. Almatrafi, N. Benajiba, M. Helal, Shelf-life, quality, safety evaluations of blueberry fruits coated with chitosan nano-material films, Sci. Rep. 11 (1) (2021) 1–10.
[26] C. Yi, H. Liu, S. Zhang, Y. Yang, Y. Zhang, Z. Lu, E. Kumacheva, Z. Nie, Self-limiting directional nanoparticle bonding governed by reaction stoichiometry, Science 369 (6509) (2020) 1369–1374.
[27] P. Sreedevi, P.S. Reddy, Effect of magnetic field and thermal radiation on natural convection in a square cavity filled with tio2 nanoparticles using tiwari-das nanofluid model, Alex. Eng. J. 61 (2) (2022) 1529–1541.
[28] P. Sudarsana Reddy, P. Sreedevi, Effect of zero mass flux condition on heat and mass transfer analysis of nanofluid flow inside a cavity with magnetic field, The European Physical Journal Plus 136 (1) (2021) 1–24.
[29] I.A. Abro, M.I. Abro, M.E. Assad, M. Rahimi-Gorji, N.M. Hoang, Investigation and evaluation of neem leaves extract as a green inhibitor for corrosion behavior of mild steel: an experimental study, Proc. IME C J. Mech. Eng. Sci. 235 (4) (2021) 734–743.
[30] I.M. Alarifi, V. Movva, M. Rahimi-Gorji, R. Asmatulu, Performance analysis of impact-damaged laminate composite structures for quality assurance, J. Braz. Soc. Mech. Sci. Eng. 41 (8) (2019) 1–16.
[31] R. Asmatulu, K.S. Erukala, M. Shinde, I.M. Alarifi, M.R. Gorji, Investigating the effects of surface treatments on adhesion properties of protective coatings on carbon fiber-reinforced composite laminates, Surf. Coating. Technol. 380 (2019), 125006.
[32] S. Abdal, U. Habib, I. Siddique, A. Akgül, B. Ali, Attribution of multi-slips and bioconvection for micropolar nanofluids transpiration through porous medium over an extending sheet with pst and phf conditions, Int. J. Algorithm. Comput. Math. 7 (6) (2021) 1–21.
[33] S. Abdal, I. Siddique, A.S. Alshomrani, F. Jarad, I.S.U. Din, S. Afzal, Significance of chemical reaction with activation energy for riga wedge flow of tangent hyperbolic nanofluid in existence of heat source, Case Stud. Therm. Eng. 28 (2021), 101542.
[34] G. Chinni, I.M. Alarifi, M. Rahimi-Gorji, R. Asmatulu, Investigating the effects of process parameters on microalgae growth, lipid extraction, and stable nanoemulsion productions, J. Mol. Liq. 291 (2019), 111308.
[35] S. Kasaragadda, I.M. Alarifi, M. Rahimi-Gorji, R. Asmatulu, Investigating the effects of surface superhydrophobicity on moisture ingression of nanofiber-reinforced bio-composite structures, Microsyst. Technol. 26 (2) (2020) 447–459.
[36] D. Habib, N. Salamat, S. Abdal, I. Siddique, M. Salimi, A. Ahmadian, On time dependent mhd nanofluid dynamics due to enlarging sheet with bioconvection and two thermal boundary conditions, Microfluid. Nanofluidics 26 (2) (2022) 1–15.
[37] S. Abdal, I. Siddique, S. Afzal, S. Sharifi, M. Salimi, A. Ahmadian, An analysis for variable physical properties involved in the nano-biofilm transportation of sutterby fluid across shrinking/stretching surface, Nanomaterials 12 (4) (2022) 599.
[38] B. Ali, S. Hussain, S.I.R. Naqvi, D. Habib, S. Abdal, Aligned magnetic and bioconvection effects on tangent hyperbolic nanofluid flow across faster/slower stretching wedge with activation energy: finite element simulation, Int. J. Algorithm. Comput. Math. 7 (4) (2021) 1–20.
[39] F. Ahmad, S. Abdal, H. Ayed, S. Hussain, S. Salim, A.O. Almatroud, The improved thermal efficiency of maxwell hybrid nanofluid comprising of graphene oxide plus silver/kerosene oil over stretching sheet, Case Stud. Therm. Eng. 27 (2021), 101257.
[40] W.A. Khan, A. Rashad, M. Abdou, I. Tlili, Natural bioconvection flow of a nanofluid containing gyrotactic microorganisms about a truncated cone, Eur. J. Mech. B Fluid 75 (2019) 133–142.

[41] N.I. Nima, M. Ferdows, O. Anwar Bég, S. Kuharat, F. Alzahrani, Biomathematical model for gyrotactic free-forced bioconvection with oxygen diffusion in near-wall transport within a porous medium fuel cell, Int. J. Biomath. (IJB) 13 (4) (2020), 2050026.
[42] M. Nayak, J. Prakash, D. Tripathi, V. Pandey, S. Shaw, O. Makinde, 3d bioconvective multiple slip flow of chemically reactive casson nanofluid with gyrotactic micro-organisms, Heat Tran. Asian Res. 49 (1) (2020) 135–153.
[43] M.A. Mansour, A.M. Rashad, B. Mallikarjuna, A.K. Hussein, M. Aichouni, L. Kolsi, Mhd mixed bioconvection in a square porous cavity filled by gyrotactic microorganisms, Int J Heat Technol 37 (2) (2019) 433–445.
[44] C.S. Balla, C. Haritha, K. Naikoti, A.M. Rashad, Bioconvection in nanofluid-saturated porous square cavity containing oxytactic microorganisms, Int. J. Numer. Methods Heat Fluid Flow 29 (4) (2019) 1448–1465.
[45] S.U. Khan, A. Rauf, S.A. Shehzad, Z. Abbas, T. Javed, Study of bioconvection flow in oldroyd-b nanofluid with motile organisms and effective Prandtl approach, Phys. Stat. Mech. Appl. 527 (2019), 121179.
[46] R.S. Saif, M. Mustafa, M.F. Afzaal, H. Assilzadeh, Analytical solutions for fluid flow triggered by a melting cylindrical surface in upper-convected maxwell (ucm) fluid, Int. Commun. Heat Mass Tran. 121 (2021), 105059.
[47] P. Sreedevi, P.S. Reddy, Williamson Hybrid Nanofluid Flow over Swirling Cylinder with Cattaneo–Christov Heat Flux and Gyrotactic Microorganism, Waves in Random and Complex Media, 2021, pp. 1–28.
[48] P. Sudarsana Reddy, K. Jyothi, M. Suryanarayana Reddy, Flow and heat transfer analysis of carbon nanotubes-based maxwell nanofluid flow driven by rotating stretchable disks with thermal radiation, J. Braz. Soc. Mech. Sci. Eng. 40 (12) (2018) 1–16.
[49] P.S. Reddy, P. Sreedevi, A.J. Chamkha, Heat and mass transfer flow of a nanofluid over an inclined plate under enhanced boundary conditions with magnetic field and thermal radiation, Heat Tran. Asian Res. 46 (7) (2017) 815–839.
[50] M. Khan, A.S. Alshomrani, et al., Characteristics of melting heat transfer during flow of carreau fluid induced by a stretching cylinder, The European Physical Journal E 40 (1) (2017) 1–9.
[51] V. Poply, P. Singh, K. Chaudhary, Analysis of laminar boundary layer flow along a stretching cylinder in the presence of thermal radiation, WSEAS Trans. Fluid Mech. 8 (4) (2013) 159–164.
[52] R. R. Rangi, N. Ahmad, Boundary Layer Flow Past a Stretching Cylinder and Heat Transfer with Variable Thermal Conductivity.